PDZ binding motif of HTLV-1 Tax promotes virus-mediated T-cell proliferation in vitro and persistence in vivo

Li Xie, Brenda Yamamoto, Abdelali Haoudi, O. John Semmes, and Patrick L. Green

HTLV-1 cellular transformation and disease induction is dependent on expression of the viral Tax oncoprotein. PDZ is a modular protein interaction domain used in organizing signaling complexes in eukaryotic cells through recognition of a specific binding motif in partner proteins. Tax-1, but not Tax-2, contains a PDZ-binding domain motif (PBM) that promotes the interaction with several cellular PDZ proteins. Herein, we investigate the contribution of the Tax-1 PBM in HTLV-induced proliferation and immortalization of primary T cells in vitro and viral survival in an infectious rabbit animal model. We generated several HTLV-1 and HTLV-2 Tax viral mutants, including HTLV-1ΔPBM, HTLV-2+C22(+PBM), and HTLV-2+C18(ΔPBM). All Tax mutants maintained the ability to significantly activate the CREB/ATF or NFκB signaling pathways. Microtiter proliferation assays revealed that the Tax-1 PBM significantly increases both HTLV-1– and HTLV-2–induced primary T-cell proliferation. In addition, Tax-1 PBM was responsible for the micronuclei induction activity of Tax-1 relative to that of Tax-2. Viral infection and persistence were severely attenuated in rabbits inoculated with HTLV-1ΔPBM. Our results provide the first direct evidence suggesting that PBM-mediated associations between Tax-1 and cellular proteins play a key role in HTLV-induced cell proliferation and genetic instability in vitro and facilitate viral persistence in vivo. (Blood. 2006;107: 1980-1988)

Introduction

HTLV-1 and HTLV-2 are highly related complex retroviruses that immortalize and transform T lymphocytes in cell culture and persist in infected individuals. However, the clinical manifestations of infection with these 2 viruses differ. HTLV-1 is associated with adult T-cell leukemia and a variety of immune-mediated disorders, including the chronic neurologic disease termed HTLV-1–associated myelopathy/tropical spastic paraparesis.[1-4] In contrast, HTLV-2 is much less pathogenic with only a few cases of variant hairy cell leukemia and neurologic disease associated with infection.[5-9]

Both HTLV-1 and HTLV-2 encode the essential Tax protein. Tax acts in *trans* to activate transcription initiation from the viral promoter.[10,11] Tax also modulates the expression or activity of various cellular factors involved in growth and differentiation and disrupts cell-cycle control and DNA repair processes.[12-14] Strong evidence suggests that these pleiotropic effects of Tax on cellular processes are required for the transforming or oncogenic capacity of HTLV.[15] Indeed, mutational analysis directly demonstrated that Tax of both HTLV-1 and HTLV-2 is essential for viral-mediated cellular transformation of primary human T cells in culture.[16-18]

Comparative studies of Tax-1 and Tax-2 revealed that these proteins display many similarities but also some major differences. Tax-1 has a higher intrinsic transactivation activity for the viral promoter than Tax-2.[19] Tax-1, but not Tax-2, is a potent inducer of micronuclei (MN) formation, which is a marker of genetic instability.[20] Tax-2, in contrast to Tax-1, fails to suppress the maturation of $CD34^+$ cells in vitro.[21] Tax-1 has been shown to inhibit p53 function more efficiently than Tax-2.[22,23] Tax-1 morphologically transforms rat fibroblasts with higher efficiency than Tax-2.[24,25] This phenotypic property was attributed to a C-terminal PDZ binding motif (PBM) that is present in Tax-1 but not Tax-2.[26] Therefore, the Tax-1 PBM could be a major determinant of the differences in pathogenicity of HTLV-1 and HTLV-2.

PDZ domain was named after the first identified PDZ-containing proteins, post-synaptic density protein (PSD-95), *Drosophila* discs large protein (DLG), and epithelial tight junction protein (Zonula Occludens-1). It is one of the protein-protein interaction modules commonly used in eukaryotic cells. A PDZ domain usually coexists in the same polypeptide either with one or multiple PDZ domains or with other protein domains such as SH3 and guanylate kinase-like domains. Through recognition of the specific carboxyl-terminal binding motif in its partner protein, PDZ domain-containing proteins play a key role in recruiting and organizing the appropriate proteins to sites of cellular signaling, as well as polar sites of cell-cell communication.[27-29]

The human homologue of DLG (hDLG), a scaffolding protein containing 3 PDZ domains, has been identified as a common target for human virus oncoproteins, including HTLV-1 Tax, adenovirus type 9 E4ORF1, and papillomavirus E6.[30-32] E6 targets hDLG for proteasome-mediated degradation, which is necessary for its transforming activity.[33-35] In contrast, Tax-1 and E4ORF1 are thought to interfere with the binding of hDLG to the adenomatous polyposis coli (APC) tumor suppressor protein via competition for

From the Department of Veterinary Biosciences, The Ohio State University; the Department of Molecular Virology, Immunology, and Medical Genetics, The Ohio State University; the Center for Retrovirus Research, The Ohio State University; the Comprehensive Cancer Center James Cancer Hospital and Solove Research Institute, The Ohio State University, Columbus; and the Department of Microbiology and Molecular Cell Biology, Eastern Virginia Medical School, Norfolk, VA.

Submitted April 1, 2005; accepted October 13, 2005. Prepublished online as *Blood* First Edition Paper, November 1, 2005; DOI 10.1182/blood-2005-03-1333.

Supported by the National Institutes of Health (grant CA93584).

An Inside *Blood* analysis of this article appears at the front of this issue.

Reprints: Patrick L. Green, The Ohio State University, 1925 Coffey Rd, Columbus, OH 43210; e-mail: green.466@osu.edu.

The publication costs of this article were defrayed in part by page charge payment. Therefore, and solely to indicate this fact, this article is hereby marked "advertisement" in accordance with 18 U.S.C. section 1734.

the same PDZ domain of hDLG. This binding leads to increased cell proliferation mediated by increased signaling through APC.[36] One study indicated that the interaction between Tax-1 and hDLG is responsible for the higher colony-forming efficiency of Rat-1 cells by Tax-1 relative to Tax-2.[26] Additional studies have implicated other cellular PDZ domain-containing proteins as Tax-1 targets, such as precursor of interleukin-16 (pro–IL-16) and a membrane-associated guanylate kinase (MAGUK) with inverted orientation (MAGI)–3. Pro–IL-16 is an abundant protein constitutively expressed in human peripheral blood T cells that can induce cell growth arrest. MAGI-3 belongs to the same MAGUK family as hDLG and has been implicated in several cellular signaling pathways involved in cell survival as well as cell polarity.[37-41] Together, these studies imply that the PBM of Tax-1 and its interacting partners, the cellular PDZ domain-containing proteins, could be a major determinant of the differences in pathogenicity of HTLV-1 and HTLV-2.

Herein, we used full-length infectious viral clones to address the role of Tax-1 PBM in the HTLV-mediated T-cell transformation process and virus survival in the rabbit model of infection. Several Tax-1 and Tax-2 viral mutants were generated, including HTLV-1 ΔPBM, HTLV-2 + C22 (Tax-2 + the last 22 amino acids of Tax-1), and HTLV-2 + C18 (ΔPBM). Tax mutants maintained the capacity to significantly activate CREB/ATF or NFκB signaling pathways. Additional analysis indicated that Tax-1 PBM is responsible for the MN induction activity (genetic instability) of Tax-1 relative to that of Tax-2. Using an in vitro coculture assay, we demonstrated that Tax-1 PBM promotes proliferation of infected T cells. Furthermore, we show that Tax-1 PBM is necessary for persistence in a rabbit model of infection. Overall, our data suggest that the interaction between Tax-1 PBM and some cellular proteins facilitates in vivo viral survival, stimulates abnormal cell proliferation, induces genetic instability, and ultimately promotes HTLV-1–mediated T-cell transformation and pathogenesis.

Materials and methods

Cells

293T, 729, and Jurkat cell lines were maintained in Dulbecco modified Eagle, Iscoves, and RPMI 1640 medium, respectively. Medium was supplemented to contain 10% FBS, 2 mM glutamine, penicillin (100 U/mL), and streptomycin (100 μg/mL). Human peripheral blood mononuclear cells (PBMCs) were isolated from blood of healthy donors by centrifugation over Ficoll-Paque (Amersham, Piscataway, NJ) and cultured in RPMI 1640 supplemented with 20% FBS, 10 U/mL IL-2 (Boehringer Mannheim, Mannheim, Germany), 2 mM glutamine, and antibiotics. The protocol for obtaining human blood was approved by The Ohio State University human subjects internal review board.

Plasmids

Tax-1 (SE356) and Tax-2 (BC20.2Sph) cDNA expression vectors were described previously.[19,42] Mutations in the *tax1* and *tax2* genes were introduced by polymerase chain reaction (PCR) mutagenesis using SE356 and BC20.2 as templates. Tax-1ΔPBM contains a 12 nucleotide deletion of the *tax1* C-terminus, resulting in loss of the last 4 amino acids of Tax-1 (ETEV), the consensus PBM. Tax-2 + C22 was generated by adding 66 nucleotides of the *tax1* coding sequence in frame to the end of *tax2*, thus adding the last 22 amino acids of Tax-1 to the shorter (331 amino acids) Tax-2A. Tax-2 + C18 was generated from Tax-2 + C22 by removing the last 4 amino acids (PBM). LTR-1–Luc, LTR-2–Luc, κB-Luc, and TK-*Renilla* were described previously.[19,43] Tax mutant viruses were generated in the HTLV-1 proviral clone (Ach), a kind gift from Lee Ratner (Washington University, St. Louis, MO)[44] or the HTLV-2 proviral clone pH6neo.[45] All mutations were confirmed by DNA sequencing.

Transfection, luciferase assay, and p19 Gag enzyme-linked immunosorbent assay (ELISA)

To measure Tax CREB/ATF-activating function, 2×10^5 293T cells were transfected using Lipofectamine PLUS (Invitrogen, Carlsbad, CA) according to the manufacturer's recommendation. The total amount of DNA was kept constant and was composed of 2 μg Tax expression vector or a negative control, 0.02 μg TK-Renilla, and 0.1 μg LTR-1– or LTR-2–Luc. To determine Tax NFκB activation capacity, 4×10^6 Jurkat cells were transfected using the Nucleofector method (Amaxa, Gaithersburg, MD) with 3 μg Tax expression vector or a negative control, 0.05 μg TK-Renilla, and 0.25 μg κB-Luc. Cell lysates were harvested 48 hours after transfection and subjected to a dual luciferase assay (Promega, Madison, WI). All experiments were performed independently 3 times in triplicate, and results were normalized for transfection efficiency using *Renilla*-Luc. Stable transfectants containing the desired proviral clones were isolated and characterized as described previously.[43]

Western blotting

Western blots were performed as recommended by the manufacturer using rabbit anti–Tax-1 or rabbit anti–Tax-2 polyclonal antisera and goat antirabbit conjugated with horseradish peroxidase. Proteins were visualized using the enhanced chemiluminescence (ECL) Western blot analysis system (Santa Cruz Biotechnology, Santa Cruz, CA).

DNA preparation, standard PCR, and quantitative Taqman real-time PCR

Genomic DNA was isolated from stable cell clones, immortalized human PBMCs, or rabbit PBMCs using PUREGENE DNA purification system (Gentra, Minneapolis, MN). DNA (1 μg) was subjected to 30-cycle PCR. Primer pair Tax8290S (^{8290}GAGCCCCAAATATCACCCG^{8308}) and TRE-AS (^{8612}CACGCTTTTATAGACTCCTG^{8593}) was used to amplify a 323-bp (base pair) fragment from wtHTLV-1 and a 311-bp fragment from HTLV-1ΔPBM, and primer pair KK1 (^{8071}CCCTCCTATCTACTCTCTC^{8089}) and LTRII-AS (^{8939}CGGGAAGACAATGCTCCTAGGGCG^{8916}) was used to amplify a 868-bp fragment from wtHTLV-2, a 934-bp fragment from HTLV-2 + C22, and a 922-bp fragment from HTLV-2 + C18. The PCR-amplified products were subjected to *Eco*RV diagnostic digestion and sequenced to confirm the PBM mutations.

For infected rabbit PBMCs, 1 μg DNA was subjected to 40-cycle PCR using primers 670 and 671[46] to amplify a 159-bp fragment specific for the HTLV-1/2 *tax/rex* region. In addition, 40 cycles of real-time Taqman PCR were conducted to quantitate proviral copy number per cell. Rabbit PBMC DNA was subjected to PCR in duplicate using the HTLV-specific primer pair AAM.001 ^{7335}CGGATACCCAGTCTACGTGTTT^{7356} and AAM.002 ^{7495}CTGAGCCGATAACGCGTCCA^{7476} and probe (5′-FAM-^{7456}ATCAC-CTGGGACCCCATCGATGGA^{7476}-TAMARA-3′), and final values were averaged. The 25-μL reactions contained 500 ng DNA, 100 ng (25 ng/mL) of each primer and probe concentration of 100 pmol/μL. Copy number was determined based on a standard curve generated from duplicate samples of dilutions of a plasmid containing the *tax* gene sequences. The copy number per cell value for a sample was generated based on the estimation that 1 μg PBMC DNA is equivalent to 67 300 cells.

Short-term coculture microtiter proliferation and long-term immortalization assays

Short-term microtiter proliferation assays were performed as described previously.[47] Briefly, freshly isolated human PBMCs were prestimulated with 2 μg/mL PHA and 10 U/mL IL-2 (Roche, Indianapolis, IN) for 3 days. 729 producer cells (2000) were irradiated with 100 Gy (10 000 rad) and cocultured with 10^4 prestimulated PBMCs in the presence of IL-2 in 96-well round-bottom plates. Wells were enumerated for growth and split 1:3 at weekly intervals. Cell proliferation was confirmed by CellTiter 96

Aqueous Non-Radioactive Cell Proliferation Assay as recommended by the manufacturer (Promega). In the modified proliferation assays, cocultures were treated with antiviral agents, 3′-azido-3′ deoxythymidine (AZT) or dextran sulfate Mr 5000 at concentrations of 10 μM or 10 μg/mL, respectively. The drugs were added to the cultures for the first time at 24 hours after plating and maintained at the same concentration with media changes every 3 days throughout the experiment. For the long-term immortalization assays, 10^6 irradiated producer cells were cocultivated with 2×10^6 freshly isolated PBMCs with 10 U/mL IL-2 in 24-well culture plates.[48] The presence of HTLV expression was confirmed by detection of p19 Gag protein in the culture supernatant at weekly intervals using a commercially available ELISA (Zeptometrix, Buffalo, NY). Viable cells were counted weekly by trypan blue exclusion. Cells inoculated with HTLV-1/2 that continued to produce p19 Gag antigen and proliferate 12 weeks after coculture in the presence of exogenous interleukin-2 (IL-2) were identified as HTLV immortalized. For each assay, at least 3 independent experiments were performed using PBMCs from distinct healthy donors.

Detection of HTLV-1/2–infected T cells by immunofluorescence analysis

Irradiated 729HTLV producer cells (10^5) were cocultured with 10^6 PBMCs in the presence of IL-2. Three days after plating, cells were washed with PAB (PBS + 0.1% NaN_3 + 1% BSA) and stained with PE-Cy5–conjugated mouse anti–human CD3 antibody. The samples were then washed, fixed, and permeabilized with Fix&Perm reagents (Serotec, Raleigh, NC). For detection of intracellular viral protein, cells were first incubated with HTLV-1/2 Gag p19 detector antibody (Zeptometrix), washed, and then incubated with fluorescein isothiocyanate (FITC)–conjugated secondary antibodies, goat anti–mouse IgG1 and goat anti–mouse IgG2b. The CD3/p19-positive cells were detected using a Leica TCS SP2 confocal microscope (Leica Microsystems, Wetzlar, Germany). 1000 cells were enumerated for each sample, and the data were presented as the percentage of infected T cells averaged over 3 independent experiments.

MN assay and cell-cycle analysis

HeLa cells were transfected with 10 μg wtTax-1, Tax-1ΔPBM, wtTax-2, Tax-2+C22 expression plasmids, or pUC19 control using the calcium phosphate transfection procedure. After 24 hours, the cultures were treated with 3 μg/mL cytochalasin B (Sigma, St Louis, MO), a cytokinesis blocking agent, and grown for an additional 30 hours. Cells were fixed with cold methanol/acetic acid (3:1) and air dried. The nuclear material was stained with a 10 μg/mL acridine orange solution for 1 minute and rinsed with dH_2O. Cells were immunostained with CREST for kinetochore identification and analyzed using a Zeiss LSM510 confocal microscope (Zeiss, Jena, Germany). Approximately 1000 cells were counted for each sample, and 2 separate experiments were performed.

For cell-cycle analysis, transfected HeLa cells were harvested using trypsin at 48 hours after transfection and then fixed in ice-cold 70% ethanol for 24 hours at 4°C. Cells were washed and resuspended in 1 mL propidium iodide solution (PBS, 50 μg/mL propidium iodide and 100 U/mL RNase A) and incubated for 30 minutes. Cells were washed, resuspended, and subjected to DNA flow cytometry analysis using a BD Biosciences (San Jose, CA) fluorescence-activated cell scanner (FACScan) with MODFIT software.

Rabbit inoculation procedures

Twelve-week-old specific pathogen-free New Zealand White rabbits (Hazelton, Kalamazoo, MI) were inoculated via the lateral ear vein with 10^7 gamma-irradiated (7500 rad) 729wtHTLV-1, 729HTLV-1ΔPBM, or 729 uninfected control cells (5 rabbits per group). This study was approved by the University Laboratory Animal Resources (ULAR) of The Ohio State University. At weeks 0, 2, 4, 6, and 8 after inoculation, 10 mL blood was drawn from the central ear artery of each animal. Serum reactivity to specific viral antigenic determinants was detected using a commercial HTLV-1 Western blot assay (Zeptometrix) adapted for rabbit plasma by use of avidin-conjugated goat anti–rabbit IgG (1:200 dilution; Sigma).[49] Serum showing reactivity to Gag (p24 or p19) and Env (gp21 or gp46) antigens was classified as positive for HTLV-1 seroreactivity.

Results

Tax-1 PBM is dispensable for Tax transcriptional activation through CREB/ATF and NFκB signaling pathways

It has been hypothesized that a PBM present at the C-terminus of Tax-1 (ETEV), but not Tax-2, may be important for the distinct pathogenic properties of HTLV-1 and HTLV-2. We generated several Tax mutants to assess directly the importance of the Tax-1 PBM in Tax function and viral oncogenic activity (Figure 1A). Tax-1ΔPBM contains a deletion of the 4 C-terminal amino acids, resulting in removal of the PBM. Tax-2 + C22 encodes a Tax-2/Tax-1 hybrid protein that contains the C-terminal 22 amino acids of Tax-1 added to the shorter Tax-2A, resulting in a protein with the equivalent length of wtTax-1. Tax-2+C18 was generated as a control and contains a deletion of the 4 C-terminal amino acids from Tax-2+C22, thereby removing the PBM. To confirm stable protein expression by each of the mutants, expression vectors were transiently transfected into 293T cells, and Tax expression was examined by Western blotting. Our results showed that the Tax mutants were expressed efficiently, with sizes consistent with peptide deletion or addition (Figure 1B). Because Tax activation of both CREB/ATF and NFκB signaling pathways plays a critical role in efficient viral replication and HTLV-mediated cellular transformation, we next tested the transactivation activity of these Tax mutants on CREB/ATF or NFκB responsive promoters. Deletion of the PBM from Tax-1 (Tax-1ΔPBM) or the addition of the PBM to Tax-2 (Tax-2+C22) had no affect on CREB/ATF activation as compared with wtTax-1 or wtTax-2 (Figure 2A). Although Tax-1 ΔPBM maintained the capacity to significantly activate NFκB, note that we consistently observed about a 50% decrease in NFκB activation activity as compared with wtTax-1, whereas Tax-2 activation of NFκB was not increased by addition of the PBM (Figure 2B).

Establishment and characterization of stable HTLV-producer cell lines

To determine the effect of Tax PBM on virus biology, mutations were transferred to their respective HTLV proviral clones, resulting in the generation of HTLV-1ΔPBM, HTLV-2+C22, and

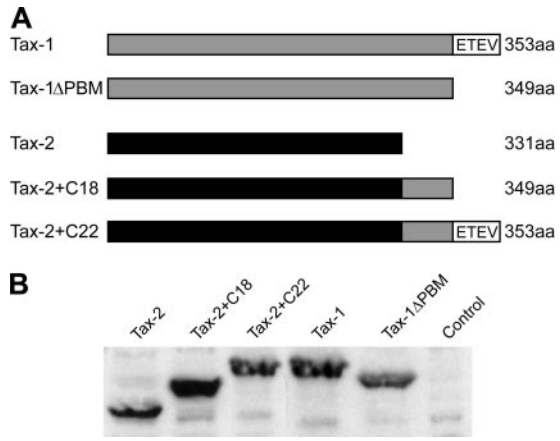

Figure 1. Structure and expression of wtTax-1, wtTax-2, and their mutant proteins. (A) Schematic representation of the Tax-1 (gray) and Tax-2A (black) constructs used in this study. The amino acid length of the proteins and sequence of the Tax-1 PBM (ETEV) are indicated. (B) Western blot of Tax-1 and Tax-2 expressed in transiently transfected 293T cells. Proteins were detected using rabbit Tax-1/Tax-2–specific antisera.

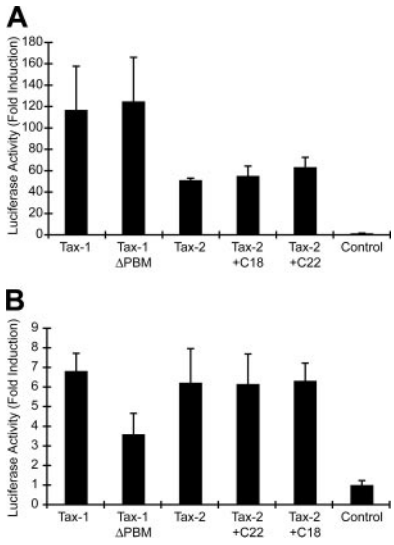

Figure 2. Tax transcriptional activation of CREB/ATF- and NFκB-dependent reporter genes. (A) 293T cells (2×10^5) were cotransfected with 2 μg Tax expression vector or a negative control, 0.02 μg TK-*Renilla*, and 0.1 μg LTR-1–Luc. Cell lysates were harvested 48 hours after transfection and subjected to a dual luciferase assay. The histogram presents the average fold activation over control values for 3 independent experiments, and error bars denote SDs. (B) Jurkat T cells (4×10^6) were cotransfected with 3 μg Tax expression vector or a negative control, 0.05 μg TK-*Renilla* and 0.25 μg κB-Luc, and luciferase activity was measured as presented in panel A.

HTLV-2+C18. We first assessed the effect of the PBM on p19 Gag production in the supernatant of transfected cells. The concentration of p19 Gag in the culture supernatant typically is used as a measure of virion production. As would be predicted from the results of our transcriptional assays, all mutant HTLV proviral clones had the capacity to produce high levels of p19 Gag, similar to the wild-type proviral clones (data not shown). Because efficient HTLV transmission is dependent on cell-to-cell contact, 729 B-cell stable transfectants expressing HTLV-1ΔPBM, HTLV-2+C22, and HTLV-2+C18 were generated and further characterized. Each of the stable transfectants contained complete copies of the provirus, and the presence of *tax* gene sequences with expected mutations was confirmed by diagnostic PCR (data not shown). To monitor the production of viral protein in these stable transfectants, the concentration of p19 Gag in the culture supernatant of several cell clones was quantified by ELISA. The amount of p19 Gag expression from each stable cell line tested was variable (Figure 3A). This likely is attributable to the chromosomal location of proviral sequences and the overall proviral copy number in the cell clones. We selected stable producer lines with p19 Gag production similar to that of our well-characterized HTLV-1 and HTLV-2 producer cell lines, 729Achneo and 729pH6neo, for assessing the ability of these mutant viruses to induce cellular proliferation and immortalization (Figure 3A). Furthermore, using Western blot, we confirmed that these lines expressed similar amounts of Tax and showed the corresponding gel mobility consistent with their altered amino acid length (Figure 3B).

Tax-1 PBM promotes HTLV-1–induced proliferation of human PBMCs

We next determined whether the Tax PBM contributed to the ability of the virus to infect and induce primary human PBMCs to proliferate. To quantify the infection and proliferation of PBMCs, 96-well microtiter assays were performed.[47] At weekly intervals, individual wells were assayed for proliferation as measured microscopically by increased cell number or by the CellTiter96 assay. A Kaplan-Meier plot of HTLV-1–induced T-cell proliferation indicated that the percentage of wells containing proliferating lymphocytes cocultured with HTLV-1ΔPBM was substantially decreased compared with cells infected with the parental HTLV-1 (9% for HTLV-1ΔPBM versus 33% for HTLV-1, Figure 4A). Although the Kaplan-Meier plot indicated that the percentage of proliferating wells were consistently increased by adding the Tax-1 PBM to the HTLV-2 Tax C-terminus, the difference was not as apparent in the HTLV-2 background (see curve for HTLV-2+C22 versus wtHTLV-2 in Figure 4B).

The measured PBM-dependent increase in cell growth observed in the microtiter assay could be attributed to a direct enhancement of proliferation of infected cells. However, another reasonable possibility is that the proliferative capacity remains constant and the Tax-1 PBM actually facilitates an increase in HTLV infectivity/spread which would result in a greater number of infected cells and ultimately increased cell growth. To distinguish between these 2 possibilities we analyzed viral infectivity of Tax wild-type or PBM mutant viruses using immunofluorescence analysis. PBMCs were cocultured with irradiated 729 viral producer B cells, and at 3 days after plating newly infected T cells ($CD3^+$, HTLV $p19^+$) were visualized and enumerated using confocal microscopy. Either deletion of Tax-1 PBM to HTLV-1 or addition of Tax-1 PBM to HTLV-2 did not significantly alter the number of HTLV p19 antigen-positive T cells as compared with wild-type HTLV (Figure 4C). Therefore, the Tax-1 PBM does not appear to alter viral infectivity.

We next performed a microtiter proliferation assay in which human PBMCs were cocultured with irradiated 729 viral producer cells, and at 1 day after coculture the medium was treated with antiviral agents (AZT or dextran sulfate) to block or limit new viral infection.[50,51] The number of proliferating cells in individual wells at 4 weeks after plating was measured by the CellTiter96 assay. Our results on control cultures (no drug) were consistent with the Kaplan-Meier plot (Figure 4A-B), indicating that the deletion of the Tax-1 PBM to HTLV-1 results in a significant decrease in proliferation (data not shown). Cultures treated with AZT or

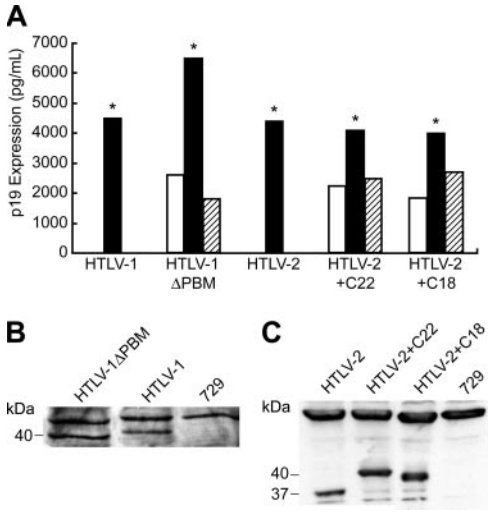

Figure 3. p19 Gag expression in permanent transfectants. (A) Three 729 stable transfectants were isolated for HTLV-1ΔPBM, HTLV-2+C22, and HTLV-2+C18 as described in "Materials and methods." Our well-established 729Achneo and 729pH6neo cell clones were used as wtHTLV-1 and wtHTLV-2 stable producer cell lines, respectively. Culture supernatants were harvested at 48 hours and tested for p19 Gag production by ELISA. Clones indicated by asterisks, which produce similar quantities of p19 Gag, were further characterized by Western blot for Tax protein expression using specific antibodies against Tax-1 (B) or Tax-2 (C), and these clones were used in subsequent experiments.

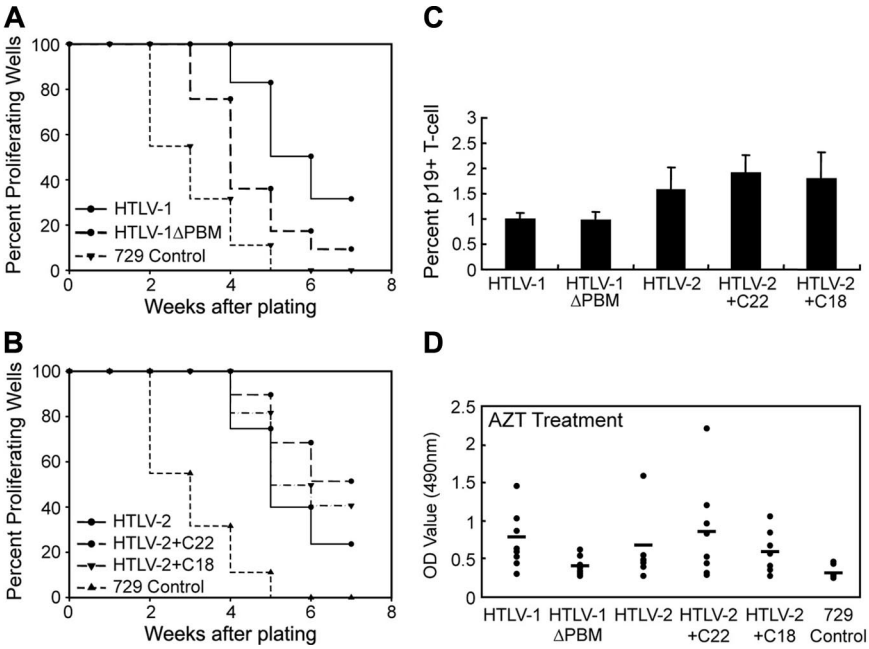

Figure 4. The Tax-1 PBM promotes HTLV-1–induced proliferation of human PBMCs. Prestimulated PBMCs (10^4) were cocultured with 2000 irradiated 729 stable producer cells in 96-well plates. The percentages of proliferating wells were plotted as a function of time (weeks). Representative Kaplan-Meier plots for wtHTLV-1 and HTLV-1ΔPBM (A), and for wtHTLV-2, HTLV-2+C22, and HTLV-2+C18 (B) are shown. (C) Tax-1 PBM does not significantly affect HTLV infectivity. The percentages of newly infected T cells ($CD3^+$, $p19^+$) were enumerated 3 days after plating by immunofluorescence analysis. The mean and SD for each sample were determined from 3 independent experiments using PBMCs from 3 different healthy donors. (D) AZT treatment did not abrogate the enhanced T-cell proliferation mediated by Tax-1 PBM. Microtiter cocultures were treated with 10 μM AZT from 24 hours after plating throughout the end of the experiment. At 4 weeks after plating, 8 random wells from each plate were subjected to the CellTiter96 proliferation assay. The OD values (λ = 490 nm) indicated in y-axis are in direct correlation with the number of proliferating cells in each well. Nontreated cocultures were set up as control. The mean values are indicated by the horizontal lines.

dextran sulfate displayed similar proliferation patterns as no drug control (Figure 4D; data not shown); T-cell proliferation was increased in the presence of the Tax-1 PBM (HTLV-1 versus HTLV-1ΔPBM, HTLV-2+C22 versus HTLV-2+C18 and HTLV-2). Taken together these results indicate that the increased growth observed in microtiter assays can be attributed to the enhanced intrinsic proliferation rate of infected cells and not increased viral infectivity or spread, supporting the conclusion that the Tax-1 PBM (ETEV) plays a critical role in HTLV-1–induced T-cell proliferation in vitro.

Tax-1 PBM is not required for HTLV-mediated immortalization of human PBMCs

To address the role of the Tax-1 PBM in HTLV-mediated human T-cell immortalization, we performed long-term coculture immortalization assays. PBMCs cocultured with 729 HTLV-1ΔPBM consistently displayed impaired or delayed growth that reached a crucial point after 6 to 7 weeks cocultivation, which is consistent with the data in the short-term proliferation assay (Figure 5A). However, the majority of the T-cell cultures survived this death crisis and eventually became immortalized. In addition, the p19 Gag production from the infected PBMCs did not fluctuate with the growth curve, and deletion of PBM did not affect viral protein production (data not shown). Similarly, HTLV-2+C22 stimulated a higher growth burst in the PBMC cocultures than wtHTLV-2 or HTLV-2+C18, especially at early infection time points (Figure 5B). In contrast to what we observed in HTLV-1–infected PBMCs, cells infected with HTLV-2+C22 continuously produced higher amounts of p19 than those infected with wtHTLV-2 or with HTLV-2+C18 (data not shown). To address whether the Tax-1 PBM affects viral protein expression, we quantified p19 Gag production from 2 cell lines newly immortalized by mutant or wild-type viruses. Our results demonstrated that p19 Gag expression was not significantly affected by either the absence of PBM in HTLV-1 or by the presence of the Tax-1 PBM in HTLV-2 (Figure 5C). We confirmed the presence of HTLV sequences and the expected Tax mutations in immortalized PBMC lines using diagnostic genome DNA PCR (Figure 5D-E). In summary, our data from short-term proliferation assays and long-term immortalization assays indicated that Tax-1 PBM can facilitate HTLV-mediated PBMC proliferation, which does not appear to alter the ability of the virus to immortalize cells.

Tax-1 PBM plays an important role in Tax induction of MN and cell-cycle control

Genetic alterations that affect the function of critical cellular machinery can result in deregulated cell-cycle progression and abnormal cellular proliferation, eventually contributing to cellular transformation. MN induction has been used as an indicator of genomic instability.[52-54] It has been shown that Tax-1 can rapidly induce MN in transfected cells, whereas Tax-2 lacks or has very limited MN induction capacity.[20,55] Our data demonstrated that Tax-1 PBM can facilitate HTLV-1–induced cellular proliferation. We next compared the relative potency of MN induction by our Tax-1 and Tax-2 mutants to determine whether the PBM is responsible for the induction of genomic instability. MN induction by wtTax-1 and wtTax-2 was consistent with previous reports, showing 4- to 5-fold and 2-fold induction, respectively, over background (Figure 6). Deletion of PBM significantly decreased Tax-1 MN induction activity to near background levels, whereas the addition of the PBM to Tax-2 resulted in a modest increase in MN but not to wtTax-1 levels (Figure 6). This result suggested that another domain of Tax-1 that is absent in Tax-2 may enhance the MN activity. Furthermore, and consistent with the MN induction/genetic instability results, cell-cycle profiles indicated that wtTax-1 expression led to the accumulation of cells in G_2/M phase (mock, 12.3%; Tax-1, 26.9%), whereas this G_2/M phase cell population was reduced significantly on deletion of PBM from Tax-1 (TaxΔPBM, 19.1%). Overall, our results suggested that PBM plays an important role in Tax-1 induction of genetic instability, which ultimately contributes to HTLV-1–mediated T-cell proliferation and transformation.

HTLV-1ΔPBM is deficient in viral survival in rabbits

To evaluate the role of the Tax-1 PBM in vivo, we compared the abilities of 729, 729HTLV-1, 729HTLV-1ΔPBM cell lines to

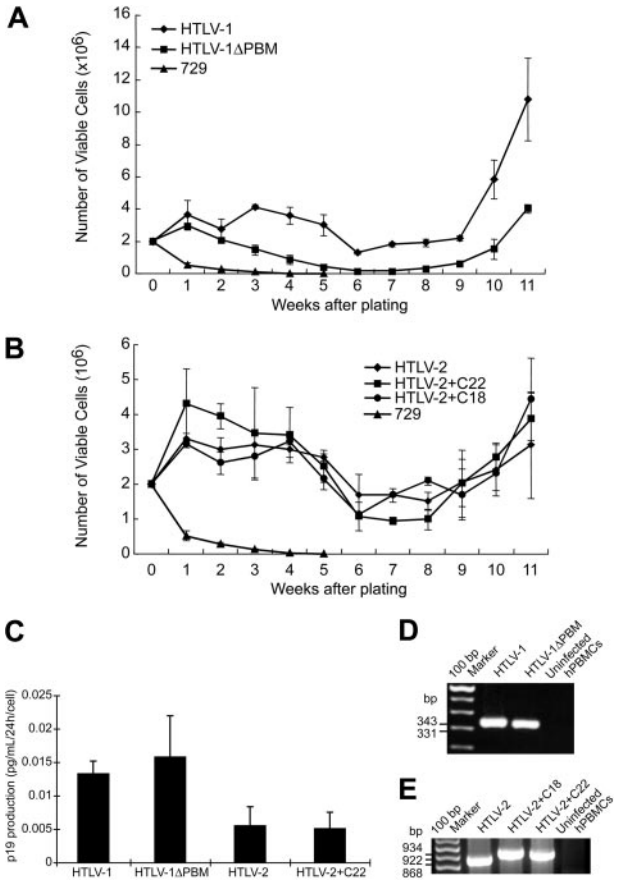

Figure 5. HTLV T-lymphocyte immortalization assays. Human PBMCs were isolated by Ficoll/Paque and cocultivated with irradiated (100 Gy [10 000 rad]) 729 stable cell lines. PBMCs (2×10^6) were cultured with irradiated donor cells (1×10^6) in 24-well plates as indicated. Representative growth curves for HTLV-1 (A) and HTLV-2 (B) infected cells are shown. Cell viability was determined weekly by trypan blue exclusion (0-11 weeks after cocultivation). The mean and SD of each time point were determined from 3 independent samples. (C) Quantification of viral protein expression from several immortalized T-lymphocyte lines established from panels A and B (20 weeks in culture). HTLV-immortalized T cells were plated in 24-well plates at 10^6 cells/mL/well. Culture supernatants were collected at 24 hours and tested for p19 Gag output by ELISA. The values represent p19 production per cell per day. The mean and SD were determined from 4 replicates of 2 independent samples. (D-E) Detection of HTLV sequences in immortalized T lymphocytes by DNA PCR. Although fragment size is consistent with the expected deletion or insertion, diagnostic restriction enzyme digestion and DNA sequencing also were performed to confirm the presence of the mutations (data not shown).

establish infection and persistence in our rabbit model. PBMCs were isolated from blood of inoculated rabbits to determine viral DNA integration by PCR, and rabbit serum was assessed for anti–HTLV-1 antibody response by Western blot. Seroconversion was detected in the 729HTLV-1–inoculated rabbits starting at week 2, and antibody titers rose over the time course of the experiment (Figure 7A). However, we were unable to detect any antibody response in rabbits inoculated with 729HTLV-1ΔPBM or 729 control.

To determine the infection status of the inoculated rabbits, amplification of specific HTLV-1 sequences from rabbit PBMCs was performed using PCR. We detected viral DNA integration in all 5 729HTLV-1–inoculated rabbits starting at week 2 after inoculation, and the viral DNA was consistently detected until the end of the experiment (Table 1). In contrast, viral DNA was detected only transiently in 2 of 5 729HTLV-1ΔPBM–inoculated rabbits at week 4 and week 6. Quantitation of the proviral copy number per cell in rabbit PBMCs by real-time PCR at 8 weeks after inoculation revealed that wtHTLV-1–inoculated rabbits contained

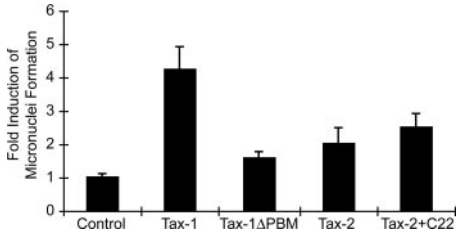

Figure 6. Tax-1 and Tax-2 induction of micronuclei. Micronuclei induction was evaluated in HeLa cells transiently transfected with cDNA expression vectors Tax-1, Tax-1ΔPBM, Tax-2, Tax-2+C22, or vector control. Cells were immunostained with CREST for kinetochore identification, and micronuclei induction was evaluated using confocal microscope. Data are presented as micronuclei counts per 1200 cells from 2 independent experiments.

approximately 0.05 to 0.08 copies per cell, whereas only the PBMCs from 1 of 5 HTLV-1ΔPBM-inoculated rabbits contained a detectable proviral load just above the limit of our assay detection sensitivity (0.003 copies per cell). Taken together, our results demonstrated that Tax-1 PBM is required for the establishment and maintenance of persistent infection in rabbits.

Discussion

Investigators have undertaken comparative studies between HTLV-1 and HTLV-2 and their gene products in an effort to understand how and why leukemogenesis is induced by HTLV-1 and only rarely by HTLV-2. Recent studies have focused on the PBM of Tax-1, not present in Tax-2, as one possible key factor in the differences in pathogenesis between HTLV-1 and HTLV-2. Indeed, the PBM of Tax-1 relative to Tax-2 has been implicated in the higher transforming activity of HTLV-1 in Rat-1 fibroblasts. This increased transforming activity has been attributed to the interaction between the Tax-1 PBM and the tumor suppressor DLG,[25,26] but it remains to be determined whether other PDZ-containing proteins also may contribute. In this study, we used full-length infectious viral clones to determine the contribution of Tax-1 PBM in the HTLV-mediated T-cell transformation process and virus survival in the rabbit model

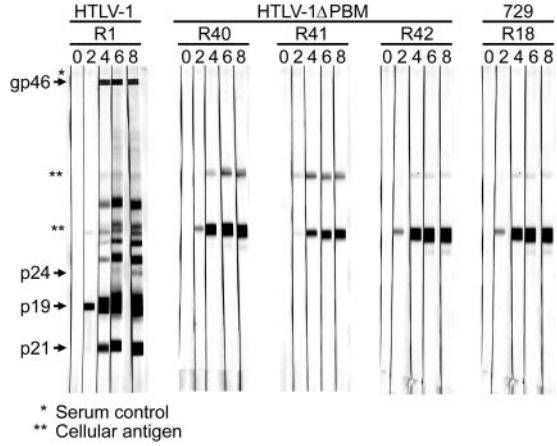

Figure 7. Assessment of HTLV-1 infection in inoculated rabbits. Rabbits were inoculated with approximately 1×10^7 irradiated 729HTLV-1, 729HTLV-1ΔPBM-infected cells, or uninfected control cells. At weeks 0, 2, 4, 6, and 8 after inoculation, rabbit PBMCs and sera were isolated from blood. HTLV-1–specific serologic response. Sera from inoculated rabbits were tested for reactivity to specific HTLV-1 proteins by Western blot. A representative rabbit from the positive wtHTLV-1–inoculated group (R1-R5) and negative control group (R18-R22), and 3 HTLV-1ΔPBM–inoculated rabbits (R40-R42) are shown. Viral proteins and 729 cell–specific proteins (**) are labeled on the left.

Table 1. PCR detection of HTLV-1 proviral sequences in inoculated rabbit PBMCs

Inoculum and rabbits	Weeks after inoculation*			
	2	4	6	8
HTLV-1				
R1	+	+	+	+
R2	+	+	+	+
R3	+	+	+	+
R4	+	+	+	+
R5	+	+	+	+
HTLV-IΔPBM				
R39	–	–	–	–
R40	–	+	–	–
R41	–	+	+	–
R42	–	–	–	–
R43	–	–	–	–
729 control				
R18	–	–	–	–

Genomic DNA was isolated from rabbit PBMCs and subjected to PCR using HTLV-1–specific primers (670-671).

+ indicates that HTLV-1 proviral sequences were detected by PCR in inoculated rabbit PBMCs; –, that HTLV-1 proviral sequences were not detected.

*All rabbits were negative at week 0.

of infection. Our data showed that deletion of the Tax-1 PBM severely disrupted the proliferation of HTLV-1–infected T lymphocytes, which also correlated with a delayed immortalization phenotype as measured in long-term coculture assays. The addition of the Tax-1 PBM to the C-terminus of Tax-2 resulted in an enhanced HTLV-2–induced T-cell proliferation. Furthermore, MN induction analysis revealed that the PBM is the major determinant of Tax-1–induced genomic instability, which correlated with an abnormal increase in the G_2/M cell-cycle profile. Finally, in vivo studies using our reproducible rabbit model of infection demonstrated the essential role of the Tax-1 PBM in efficient HTLV-1 persistence.

To date, 3 PDZ-containing proteins, hDLG, MAGI-3, and pro–IL-16, which have been implicated in either tumor suppression or cell-cycle regulation, have been demonstrated to interact with Tax-1 via their respective PDZ domains.[30,32,37,41] The hDLG interacts with APC, and a functional APC-hDLG complex is required to efficiently block cell-cycle progression from G_0/G_1 to S phase. Tax-1 has been shown to bind to the same PDZ domain of hDLG as APC, thereby competing with APC for hDLG binding and releasing the cell-cycle inhibition by this complex.[36] A recent study by Wu et al[38] suggested that the PDZ domain–mediated association between MAGI-3 and a tumor suppressor, "phosphatase with tensin homology mutated in multiple advanced cancers" (PTEN/MMAC), performs a critical role in bringing PTEN/MMAC to proper subcellular sites, allowing for enhanced regulation of certain signaling pathway involved with cell survival. Similarly, Tax-1 PBM could disrupt the function of PTEN/MMAC by competing for binding to the MAGI-3 PDZ-domain.[38] Pro–IL-16, which is expressed constitutively in human $CD4^+$ T cells (the target for HTLV-1 malignancy), contains 3 PDZ motifs that are highly homologous to hDlg. Tax-1 interacts with the first PDZ domain of pro–IL-16 and eliminates the G_0/G_1 cell-cycle arrest function mediated by pro–IL-16.[37] These results, taken together with ours, strongly support the conclusion that the Tax-1 PBM enhances T-cell proliferation and viral survival in the infected host possibly by disrupting cell partners important for cell-cycle and apoptosis regulatory control.

An interesting observation is that viral infection and persistence in HTLV-1ΔPBM–inoculated rabbits were severely attenuated. In contrast, wtHTLV-2 that does not contain a Tax PBM can successfully persist in rabbits. The underlying mechanism for this discrepancy is unclear but likely resides in one of the genetic/biologic differences between HTLV-1 and HTLV-2.[56] For example, both Tax-1 and Tax-2 have been shown to protect cells from apoptosis. Although Tax-1 inhibits apoptosis by up-regulation of Bcl-2 and repression of Bax, Tax-2 has been shown to protect cells from Fas-mediated apoptosis by up-regulation of Bcl-XL expression. Moreover, it appears that Tax-1 can confer resistance to apoptosis from a broad range of apoptosis stimuli, including DNA damage. It is possible that deletion of PBM from Tax-1 affects its capacity of apoptosis inhibition, and thus disrupts the balance between cell death and cell growth of HTLV-1–infected cells. Specifically, PBM-mediated association between Tax-1 and MAGI-3 has been implicated into the apoptosis regulatory control. In contrast, Tax-2 can provide cell survival signal even in the absence of PBM. Therefore, HTLV-2 can achieve the successful viral replication and persistence in inoculated rabbits, whereas the in vivo survival of HTLV-1ΔPBM is severely impaired. In this respect, the attenuated cell proliferation mediated by HTLV-1ΔPBM observed in in vitro microtiter assay may be the manifestation of decreased survival of infected cells.

In in vitro immortalization assays, HTLV-1ΔPBM–cocultured PBMCs consistently showed a decreased growth pattern compared with those cocultured with wtHTLV-1. In contrast, the Tax-1 PBM in the context of HTLV-2 (HTLV-2+C22) resulted in a slight increase in growth of infected PBMCs at the early stage of infection. Furthermore, addition of the Tax-1 PBM to Tax-2 (Tax-2+C22) could not completely rescue its activity to induce micronuclei and disrupt cell cycle to the level of wtTax-1. One explanation could be that the function of Tax-1 PBM is different in the context of Tax-2 versus the context of Tax-1. Originally, both Tax-1 and Tax-2 were regarded as nuclear proteins that colocalized primarily with RNA polymerase II, splicing complexes, and specific transcription factors.[57,58] More recently, studies have shown that Tax-1 is a shuttling protein with a primary localization at the nuclear speckled structure, whereas Tax-2 is mainly localized in the cytoplasm.[59-61] Therefore, it is possible that Tax-1 PBM primarily associates with some nuclear proteins in the context of Tax-1, but mainly complexes with some cytoplasmic proteins in the context of Tax-2. This may also explain why Tax transcriptional activation of NFκB was decreased by deletion of PBM from Tax-1 but not increased by addition of PBM to Tax-2. However, this difference is not exclusive, because HTLV-2–induced cell proliferation was improved in the presence of PBM in the short-term proliferation assay.

In summary, the associations between Tax-1 and cellular proteins mediated by PBM can induce genetic instability, stimulate abnormal cell-cycle progression and cellular proliferation, facilitate in vivo viral infection, and ultimately promote HTLV-1–induced T-cell transformation and pathogenesis.

Acknowledgments

We thank A. Phipps, I. Younis, and J. Arnold for their assistance with the rabbit experiments. We also thank Tim Vojt for preparation of the figures and Kate Hayes for editorial comments.

References

1. Green PL, Chen ISY. Human T-cell leukemia virus types 1 and 2. In: Knipe DM, Howley P, Griffin D, Lamb R, Martin M, Straus S, eds. Virology. 4th ed. Philadelphia. PA: Lippincott Williams & Wilkins; 2001: 1941-1969.
2. Manns A, Hisada M, La Grenade L. Human T-lymphotropic virus type I infection. Lancet. 1999; 353:1951-1958.
3. Osame M, Usuku K, Izumo S, et al. HTLV-I-associated myelopathy: a new clinical entity. Lancet. 1986;1:1031-1032.
4. Takatsuki K, Yamaguchi K, Kawano F, et al. Clinical diversity in adult T-cell leukemia/lymphoma. Cancer Res. 1985;45(9 suppl):4644s-4645s.
5. Rosenblatt JD, Giorgi JV, Golde DW, et al. Integrated human T-cell leukemia virus II genome in $CD8^+$ T cells from a patient with "atypica" hairy cell leukemia: evidence for distinct T and B cell lymphoproliferative disorders. Blood. 1988;71: 363-369.
6. Berger JR, Svenningsson A, Raffanti S, Resnick L. Tropical spastic paraparesis-like illness occurring in a patient dually infected with HIV-1 and HTLV-II. Neurology. 1991;41:5-7.
7. Hjelle B, Appenzeller O, Mills R, et al. Chronic neurodegenerative disease associated with HTLV-II infection. Lancet. 1992;339:645-646.
8. Harrington WJ Jr, Sheremata W, Hjelle B, et al. Spastic ataxia associated with human T-cell lymphotropic virus type II infection. Annals Neurol. 1993;7:1031-1034.
9. Poiesz B, Dube D, Dube S, et al. HTLV-II-associated cutaneous T-cell lymphoma in a patient with HIV-1 infection. N Engl J Med. 2000; 342:930-936.
10. Felber BK, Paskalis H, Kleinman-Ewing C, Wong-Staal F, Pavlakis GN. The pX protein of HTLV-I is a transcriptional activator of its long terminal repeats. Science. 1985;229:675-679.
11. Fujisawa J, Seiki M, Kiyokawa T, Yoshida M. Functional activation of the long terminal repeat of human T-cell leukemia virus type I by a trans-acting factor. Proc Natl Acad Sci U S A. 1985;82: 2277-2281.
12. Kehn K, Berro R, de la Fuente C, et al. Mechanisms of HTLV-1 transformation. Front Biosci. 2004;9:2347-2372.
13. Yoshida M. Multiple viral strategies of HTLV-1 for dysregulation of cell growth control. Annu Rev Immunol. 2001;19:475-496.
14. Wycuff DR, Marriott SJ. The HTLV-1 Tax oncoprotein: hypertasking at the molecular level. Front Biosci. 2005;10:620-642.
15. Gatza ML, Watt JC, Marriott S. Cellular transformation by the HTLV-I Tax protein, a jack-of-all-trades. Oncogene. 2003;22:5141-5149.
16. Robek MD, Ratner L. Immortalization of $CD4^+$ and $CD8^+$ T-lymphocytes by human T-cell leukemia virus type 1 Tax mutants expressed in a functional molecular clone. J Virol. 1999;73:4856-4865.
17. Ross TM, Pettiford SM, Green PL. The *tax* gene of human T-cell leukemia virus type 2 is essential for transformation of human T lymphocytes. J Virol. 1996;70:5194-5202.
18. Ross TM, Narayan M, Fang ZY, Minella AC, Green PL. Tax transactivation of both $NF\kappa B$ and CREB/ATF is essential for human T-cell leukemia virus type 2-mediated transformation of primary human T-cells. J Virol. 2000;74: 2655-2662.
19. Ye J, Xie L, Green PL. Tax and overlapping Rex sequences do not confer the distinct transformation tropisms of HTLV-1 and HTLV-2. J Virol. 2003;77:7728-7735.
20. Semmes OJ, Majone F, Cantemir C, Turchetto L, Hjelle B, Jeang KT. HTLV-I and HTLV-II Tax: differences in induction of micronuclei in cells and transcriptional activation of viral LTRs. Virology. 1996;217:373-379.
21. Tripp A, Liu Y, Sieburg M, Montalbano J, Wrzesinski S, Feuer G. Human T-cell leukemia virus type 1 tax oncoprotein suppression of multilineage hematopoiesis of $CD34^+$ cells in vitro. J Virol. 2003; 77:12152-12164.
22. Mahieux R, Pise-Masison CA, Lambert PF, et al. Differences in the ability of human T-cell lymphotropic virus type 1 (HTLV-1) and HTLV-2 tax to inhibit p53 function. J Virol. 2000;74: 6866-6874.
23. Van PL, Yim KW, Jin DY, Dapolito G, Kurimasa A, Jeang KT. Genetic evidence of a role for ATM in functional interaction between human T-cell leukemia virus type 1 Tax and p53. J Virol. 2001;75: 396-407.
24. Pozzatti R, Vogel J, Jay G. The human T cell lymphotropic virus type I tax gene can cooperate with the ras oncogene to induce neoplastic transformation of cells. Mol Cell Biol. 1990;10: 413-417.
25. Endo K, Hirata A, Iwai K, et al. Human T-cell leukemia virus type 2 (HTLV-2) Tax protein transforms a rat fibroblast cell line but less efficiently than HTLV-1 Tax. J Virol. 2002;76:2648-2653.
26. Hirata A, Higuchi M, Niinuma A, et al. PDZ domain-binding motif of human T-cell leukemia virus type 1 Tax oncoprotein augments the transforming activity in a rat fibroblast cell line. Virology. 2004;318:327-336.
27. Fanning AS, Anderson JM. Protein modules as organizers of membrane structure. Curr Opin Cell Biol. 1999;11:432-439.
28. Harris BZ, Lim WA. Mechanism and role of PDZ domains in signaling complex assembly. J Cell Sci. 2001;114:3219-3231.
29. Sheng M, Sala C. PDZ domains and the organization of supramolecular complexes. Annu Rev Neurosci. 2001;24:1-29.
30. Suzuki T, Ohsugi Y, Uchida-Toita M, Akiyama T, Yoshida M. Tax oncoprotein of HTLV-1 binds to the human homologue of Drosophila discs large tumor suppressor protein, hDLG, and perturbs its function in cell growth control. Oncogene. 1999; 18:5967-5972.
31. Rousset R, Fabre S, Desbois C, Bantignies F, Jalinot P. The C-terminus of the HTLV-1 Tax oncoprotein mediates interaction with the PDZ domain of cellular proteins. Oncogene. 1998;16: 643-654.
32. Lee SS, Weiss RS, Javier RT. Binding of human virus oncoproteins to hDlg/SAP97, a mammalian homolog of the Drosophila discs large tumor suppressor protein. Proc Natl Acad Sci U S A. 1997; 94:6670-6675.
33. Gardiol D, Kuhne C, Glaunsinger B, Lee SS, Javier R, Banks L. Oncogenic human papillomavirus E6 proteins target the discs large tumour suppressor for proteasome-mediated degradation. Oncogene. 1999;18:5487-5496.
34. Watson RA, Thomas M, Banks L, Roberts S. Activity of the human papillomavirus E6 PDZ-binding motif correlates with an enhanced morphological transformation of immortalized human keratinocytes. J Cell Sci. 2003;116:4925-4934.
35. Lee C, Laimins LA. Role of the PDZ domain-binding motif of the oncoprotein E6 in the pathogenesis of human papillomavirus type 31. J Virol. 2004;78:12366-12377.
36. Ishidate T, Matsumine A, Toyoshima K, Akiyama T. The APC-hDLG complex negatively regulates cell cycle progression from the G0/G1 to S phase. Oncogene. 2000;19:365-372.
37. Wilson KC, Center DM, Cruikshank WW, Zhang Y. Binding of HTLV-1 tax oncoprotein to the precursor of interleukin-16, a T cell PDZ domain-containing protein. Virology. 2003;306:60-67.
38. Wu Y, Dowbenko D, Spencer S, et al. Interaction of the tumor suppressor PTEN/MMAC with a PDZ domain of MAGI3, a novel membrane-associated guanylate kinase. J Biol Chem. 2000;275:21477-21485.
39. Adamsky K, Arnold K, Sabanay H, Peles E. Junctional protein MAGI-3 interacts with receptor tyrosine phosphatase beta (RPTP beta) and tyrosine-phosphorylated proteins. J Cell Sci. 2003; 116:1279-1289.
40. Yao R, Natsume Y, Noda T. MAGI-3 is involved in the regulation of the JNK signaling pathway as a scaffold protein for frizzled and Ltap. Oncogene. 2004;23:6023-6030.
41. Ohashi M, Sakurai M, Higuchi M, et al. Human T-cell leukemia virus type 1 Tax oncoprotein induces and interacts with a multi-PDZ domain protein, MAGI-3. Virology. 2004;320:52-62.
42. Green PL, Xie Y, Chen ISY. The Rex proteins of human T-cell leukemia virus type-II differ by serine phosphorylation. J Virol. 1991;65:546-550.
43. Ye J, Sileverman L, Lairmore MD, Green PL. HTLV-1 Rex is required for viral spread and persistence in vivo but is dispensable for cellular immortalization in vitro. Blood. 2003;102:3963-3969.
44. Kimata JT, Wong FH, Wang JJ, Ratner L. Construction and characterization of infectious human T-cell leukemia virus type I molecular clones. Virology. 1994;204:656-664.
45. Chen IY, McLaughlin J, Gasson JC, Clark SC, Golde DW. Molecular characterization of genome of a novel human T-cell leukaemia virus. Nature. 1983;305:502-505.
46. Kusuhara K, Anderson M, Pettiford SM, Green PL. Human T-cell leukemia virus type 2 Rex protein increases stability and promotes nuclear to cytoplasmic transport of *gag/pol* and *env* RNAs. J Virol. 1999;73:8112-8119.
47. Persaud D, Munoz JL, Tarsis SL, Parks ES, Parks WP. Time course and cytokine dependence of human T-cell lymphotropic virus type 1 T-lymphocyte transformation as revealed by a microtiter infectivity assay. J Virol. 1995;69: 6297-6303.
48. Green PL, Ross TM, Chen ISY, Pettiford S. Human T-cell leukemia virus type II nucleotide sequences between *env* and the last exon of *tax/rex* are not required for viral replication or cellular transformation. J Virol. 1995;69:387-394.
49. Collins ND, Newbound GC, Albrecht B, Beard J, Ratner L, Lairmore MD. Selective ablation of human T-cell lymphotropic virus type 1 p12I reduces viral infectivity in vivo. Blood. 1998;91: 4701-4707.
50. Baba M, Pauwels R, Balzarini J, Arnout J, Desmyter J, De Clercq E. Mechanism of inhibitory effect of dextran sulfate and heparin on replication of human immunodeficiency virus in vitro. Proc Natl Acad Sci U S A. 1988;85:6132-6136.
51. Macchi B, Faraoni I, Zhang J, et al. AZT inhibits the transmission of human T cell leukaemia/lymphoma virus type I to adult peripheral blood mononuclear cells in vitro. J Gen Virol. 1997;78 (Pt 5):1007-1016.
52. Fenech M, Morley AA. Measurement of micronuclei in lymphocytes. Mutat Res. 1985;147:29-36.

53. Parry EM, Parry JM, Corso C, et al. Detection and characterization of mechanisms of action of aneugenic chemicals. Mutagenesis. 2002; 17:509-521.
54. Norppa H, Falck GC. What do human micronuclei contain? Mutagenesis. 2003;18:221-233.
55. Majone F, Semmes OJ, Jeang K-T. Induction of micronuclei by HTLV-I Tax: a cellular assay for function. Virology. 1993;193:456-459.
56. Feuer G, Green PL. Comparative biology of human T-cell lynphotropic virus type 1 (HTLV-1) and HTLV-2. Oncogene. 2005;24:5996-6004.
57. Bex F, McDowall A, Burny A, Gaynor RB. The human T-cell leukemia virus type 1 transactivator protein Tax colocalizes in unique nuclear structures with NFκB proteins. J Virol. 1997;71:3484-3497.
58. Goh WC, Sodroski J, Rosen C, Essex M, Haseltine WA. Subcellular localization of the product of the long open reading frame of human T-cell leukemia virus type I. Science. 1985;227: 1227-1228.
59. Semmes O, Jeang K. Localization of human T-cell leukemia virus type 1 Tax to subcellular compartments that overlap with interchromatin speckles. J Virol. 1996;70:6347-6357.
60. Burton M, Upadhyaya CD, Maier B, Hope TJ, Semmes OJ. Human T-cell leukemia virus type 1 Tax shuttles between functionally discrete subcellular targets. J Virol. 2000;74:2351-2364.
61. Meertens L, Chevalier S, Weil R, Gessain A, Mahieux R. A 10-amino acid domain within human T-cell leukemia virus type 1 and type 2 tax protein sequences is responsible for their divergent subcellular distribution. J Biol Chem. 2004; 279:43307-43320.